Supporting Information

Magnetic Fe NPs as Peroxidase Nanozyme for Sensitive and Rapid Colorimetric Monitoring of H_2O_2 and Xanthine

Yan Wu [a, b]*, Mengjie He [a], Honghui Zang [c], Junli Wang [a], Jing Li [a], Ting Yue [a], Rong Xu [a], Yueshan Jiang [a], Fang Zhao [a] and Siyi Chen [a]

[a] *Chongqing Key Laboratory of Inorganic Special Functional Materials, College of Chemistry and Chemical Engineering, Yangtze Normal University, Fuling, Chongqing 408100, China*

[b] *Postdoctoral mobile station of Basic Medical Sciences, Hengyang Medical School, University of South China, Hengyang 421001, China*

[c] *Chongqing Wankai New Materials Technology Co., Ltd, Fuling, Chongqing 408121, China.*

* To whom correspondence should be addressed.

E-mail: wyan2018@163.com, Tel＆Fax: +86-0734-8282133

Materials and apparatus

Iron(III) chloride hexahydrate ($FeCl_3.6H_2O$), xanthine, and sodium borohydride ($NaBH_4$) were obtained from Aladdin Reagent Co., Ltd. (Shanghai, China). Xanthine oxidase (XOD) and ascorbic acid were obtained from Shanghai Yuanye Biological Technology Co., Ltd. (Shanghai, China). Glucose, L-cysteine, uric acid, L-lysine, cholesterol, L-tyrosine, D-fructose, lactose, D-maltose monohydrate, glutathione, $NaHPO_4^{3-}$, and H_2O_2 were bought from Shanghai Titan Technology Co., Ltd. (Shanghai, China). TMB was purchased from Adamas Reagent Co., Ltd. (Shanghai, China), 2',7'-dichlorofluorescein (DCF) was purchased from Macklin Biochemical Co., Ltd (Shanghai, China). Thiourea, *p*-benzoquinone, and NaN_3 were purchased from Kelong Chemical Reagent Co., Ltd. (Chengdu, China). All the human serum samples were achieved from the School Hospital.

The XRD was performed on a D/MAX-2500 (Rigaku, USA). The XPS study was conducted by K-ALPHA (Thermo Fisher Scientific, U.K.). A Hitachi U-4100 spectrometer (Japan) was used to record UV-vis absorption spectra. Magnetic Fe NPs were characterized using a FEI Tecnai G2 F20 transmission electron microscope (TEM). The magnetic performance of Fe NPs was researched by a PPMS-9T vibrating-sample magetometer (USA). Radical signals were measured by electron spin resonance (ESR, Bruker EMXplus).

Preparation of Fe NPs

According to the reported method,[1] the synthesis procedure of magnetic Fe NPs was as follows: typically, 0.6768 g of $FeCl_3 \cdot 6H_2O$ and 0.2891 g of $NaBH_4$ were dispersed in 100 mL ddH_2O, respectively. The $NaBH_4$ solution was quickly added to the $FeCl_3$ solution. Subsequently, the mixed solution was stirred and reacted for 1 h. The obtained black outcome was washed with ddH_2O and ethanol, respectively. At last, the obtained product was dried at 60 °C for 8 h, and saved in a dry environment for subsequent experiments.

The operation of reusability experiment in Figure S8B

The reusability experiment was performed under the same conditions of the analysis (pH 3.5 NaAc-HAc buffer, Fe NPs 1 mg/mL, H_2O_2 100 μM, TMB 5mM, react at room temperature, reaction time 10 min). The volume of reaction system was enlarged for 300 times from 3.0 mL to 900 mL. After reaction for 10 min, the Fe NPs was collected with magnet and washed by ethanol for twice and then dried at 60 ^{o}C under vacuum condition. About 4.0 mg power could be collected. The collected Fe NPs nanozyme can be employed for the second cycle in detection of H_2O_2.

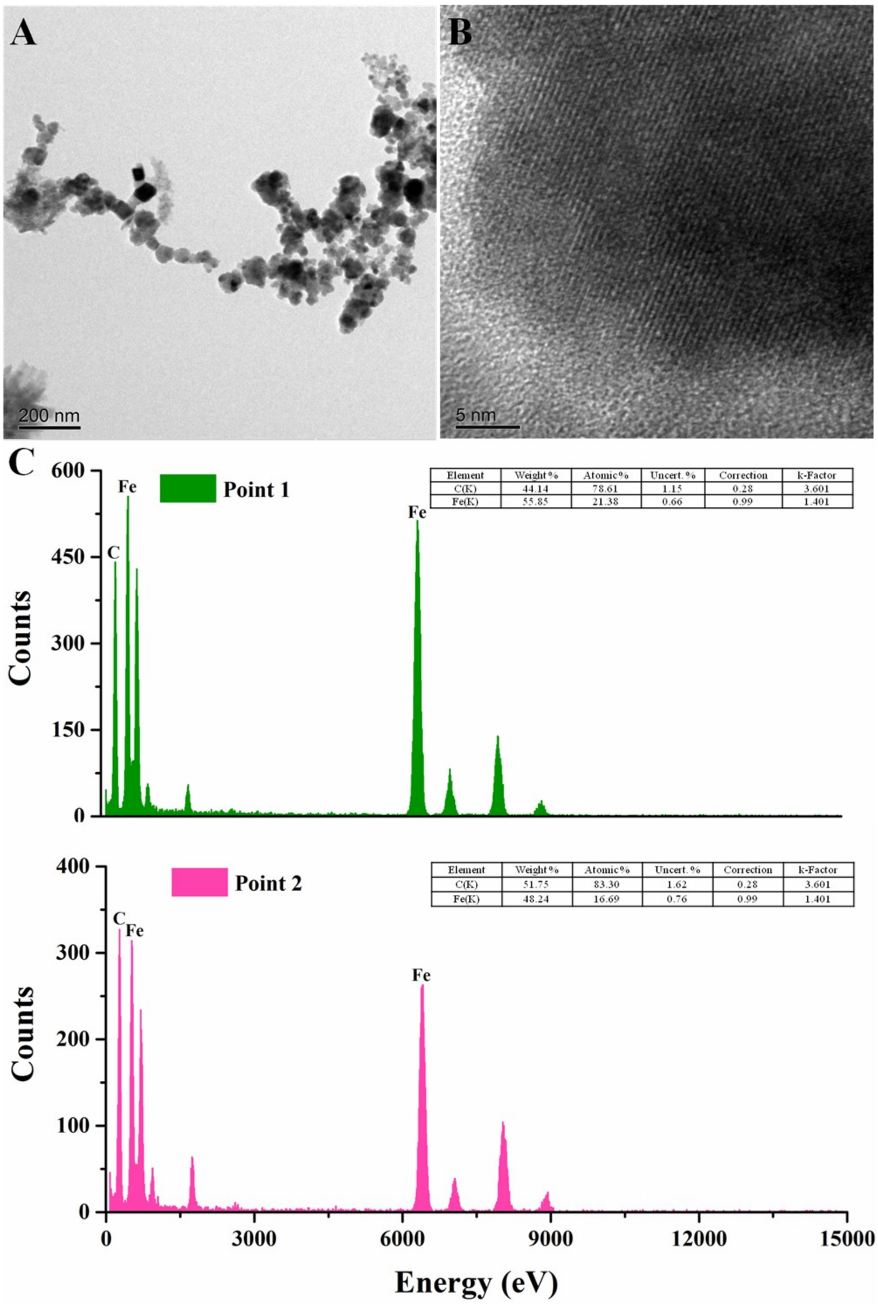

Element	Weight%	Atomic%	Uncert.%	Correction	k-Factor
C(K)	44.14	78.61	1.15	0.28	3.601
Fe(K)	55.85	21.38	0.66	0.99	1.401

Element	Weight%	Atomic%	Uncert.%	Correction	k-Factor
C(K)	51.75	83.30	1.62	0.28	3.601
Fe(K)	48.24	16.69	0.76	0.99	1.401

Figure S1. (a) TEM and (b) HRTEM images of Fe NPs. (c) EDX spectra of different points of outer shell of Fe NPs.

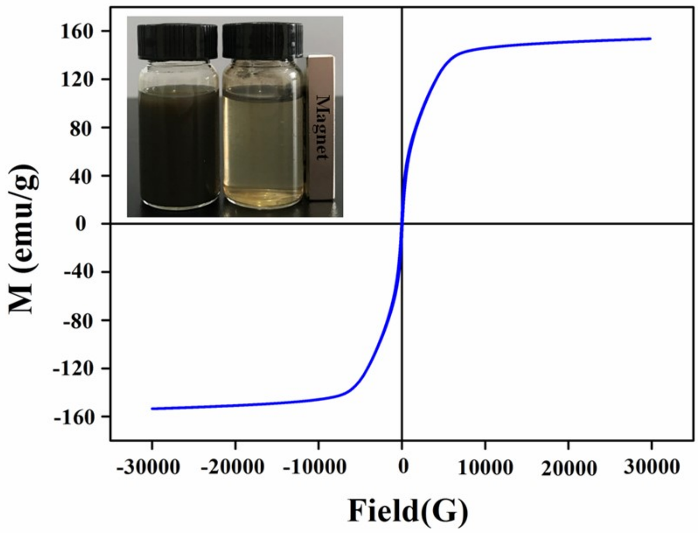

Figure S2. Magnetic hysteresis curve of Fe NPs. Inset: pictures of Fe NPs in solution with and without a magnet.

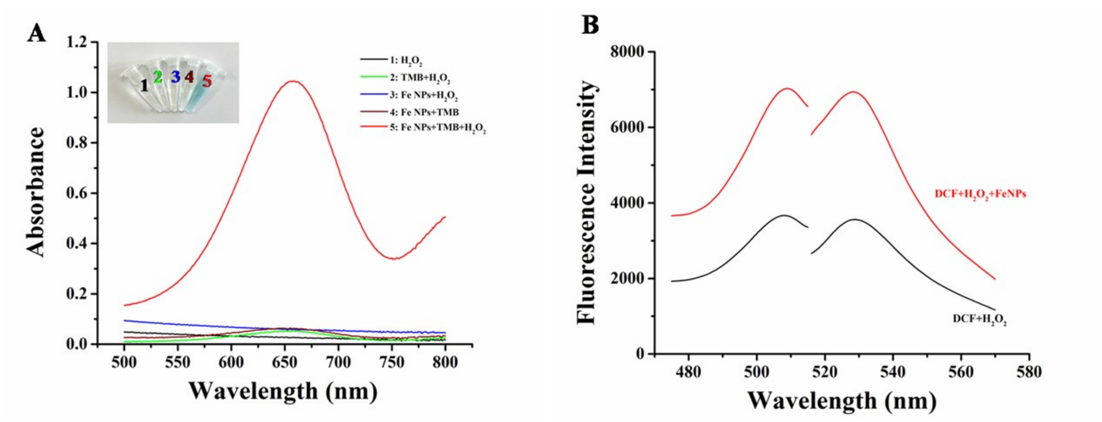

Figure S3. (A) Absorption spectra of H_2O_2, TMB + H_2O_2, Fe NPs nanozyme + H_2O_2, Fe NPs nanozyme + TMB , and Fe NPs nanozyme + TMB + H_2O_2. Inset is the corresponding photographs of five reactions (from left to right): H_2O_2, TMB + H_2O_2, Fe NPs nanozyme + H_2O_2, Fe NPs nanozyme + TMB , and Fe NPs nanozyme + TMB + H_2O_2. (B) Excitation and emission spectra of DCF in the presence of Fe NPs nanozyme (red line) and absence of Fe NPs nanozyme (black line).

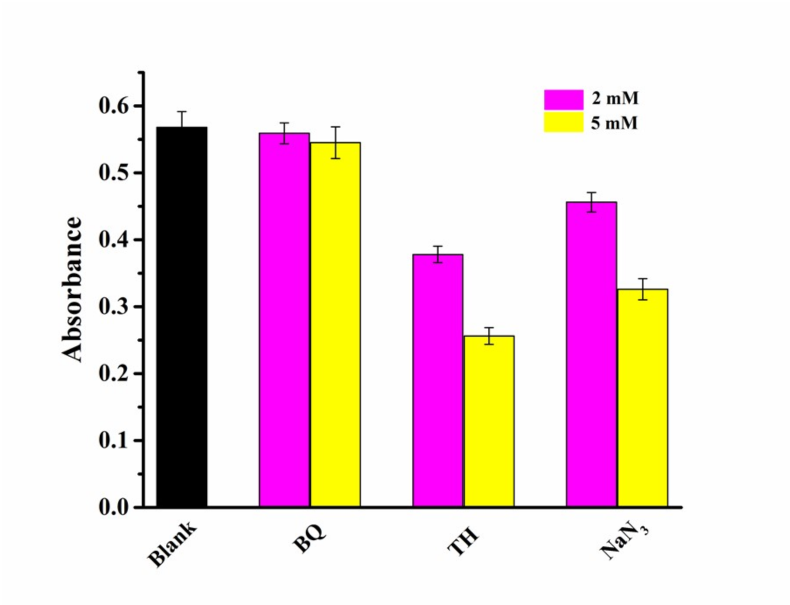

Figure S4. A_{652} variance of the TMB/H_2O_2/Fe NPs system in the presence of BQ, TH, and NaN_3.

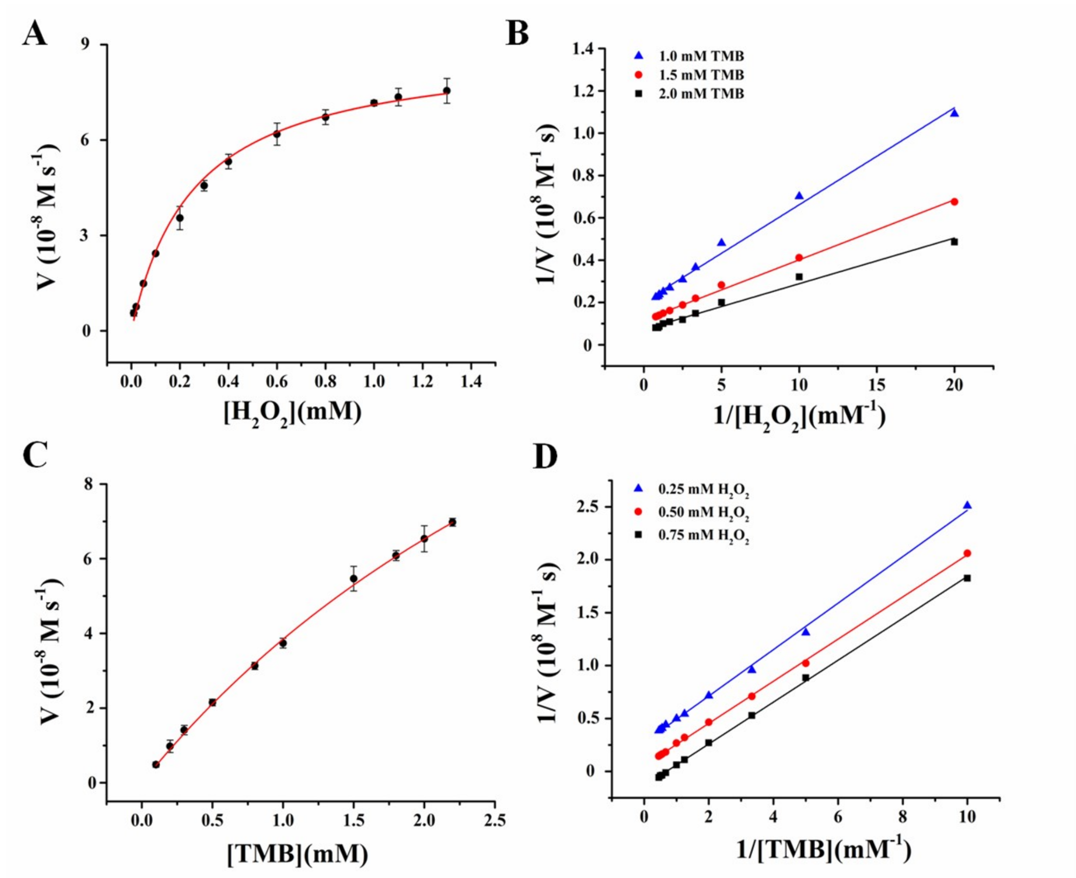

Figure S5. An analysis of the steady-state kinetics of the Fe NPs-based catalytic system employing the Michaelis-Menten model (A and C) and Lineweaver-Burk double-reciprocal model (B and D). (A) Reaction velocity plots with a unchanged TMB concentration (1.5 mM) and H_2O_2 concentration changed. (C) Reaction velocity plots with a unchanged H_2O_2 concentration (0.5 mM) and TMB concentration varied. (B) and (D) Double reciprocal plots of the catalytic system with the content of one substrate (H_2O_2 or TMB) changed. The catalytic system was performed at pH 3.5 with 1 mg.mL^{-1} of Fe NPs.

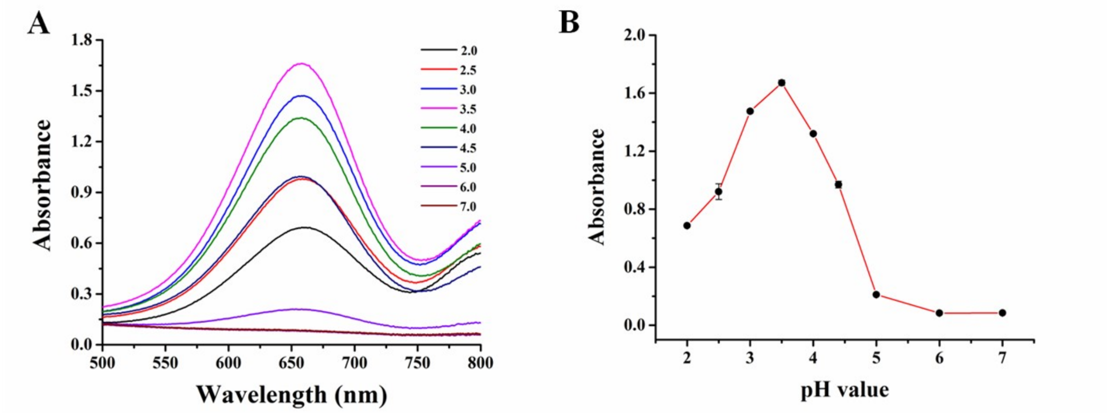

Figure S6. UV-vis absorption spectra of (A) pH value of Fe NPs nanoenzyme. Optimum conditions for xanthine response based on the Fe NPs nanozyme sensing platform. (B) pH value of the Fe NPs nanozyme. The error bar represents the deviation of three determinations.

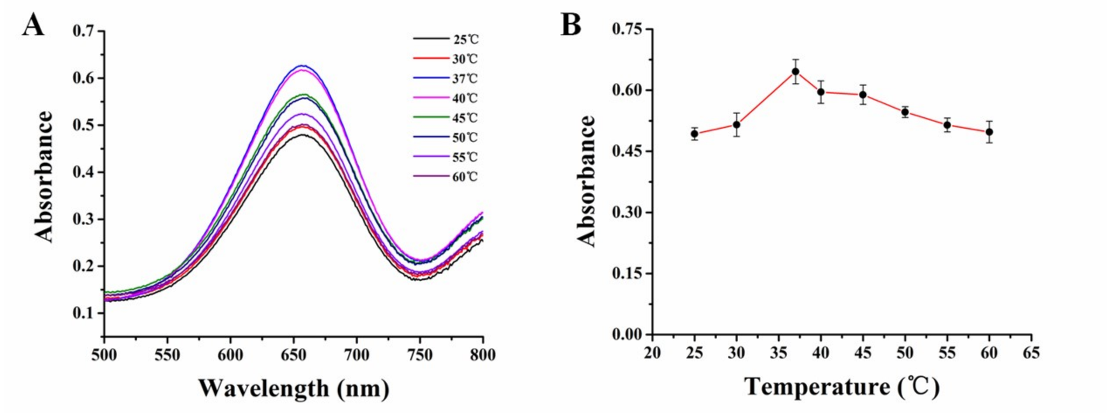

Figure S7. UV-vis absorption spectra of (A) incubation temperature between XOD and xanthine. Optimum conditions for xanthine response based on the Fe NPs nanozyme sensing platform. (B) incubation temperature between XOD and xanthine. The error bar represents the deviation of three determinations.

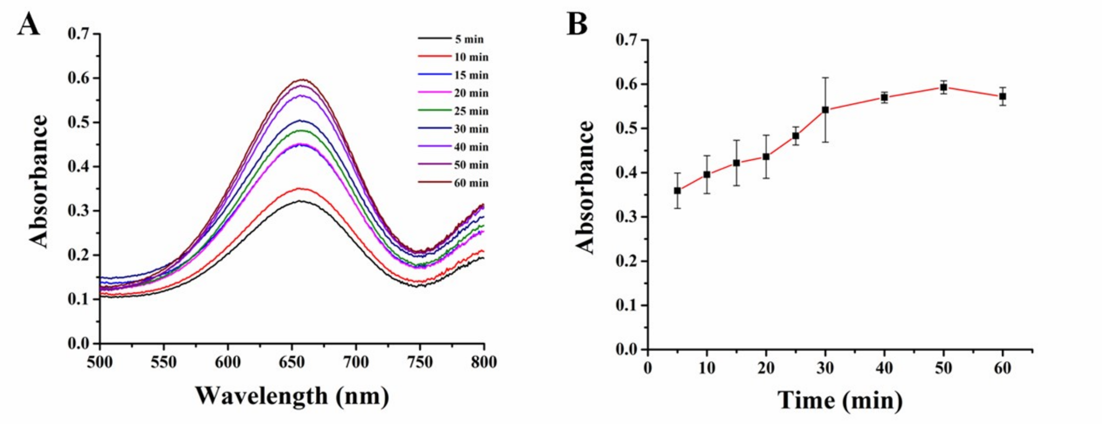

Figure S8. UV-vis absorption spectra of (A) incubation time between XOD and xanthine. Optimum conditions for xanthine response based on the Fe NPs nanozyme sensing platform. (B) incubation time between XOD and xanthine. The error bar represents the deviation of three determinations.

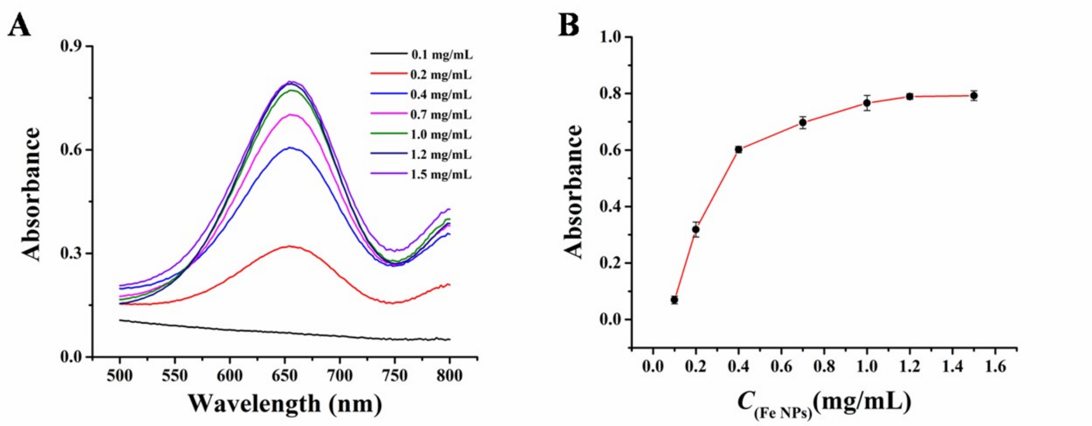

Figure S9. UV-vis absorption spectra of (A) concentration of Fe NPs nanozyme. Optimum conditions for xanthine response based on the Fe NPs nanozyme sensing platform. (B) concentration of Fe NPs nanozyme. The error bar represents the deviation of three determinations.

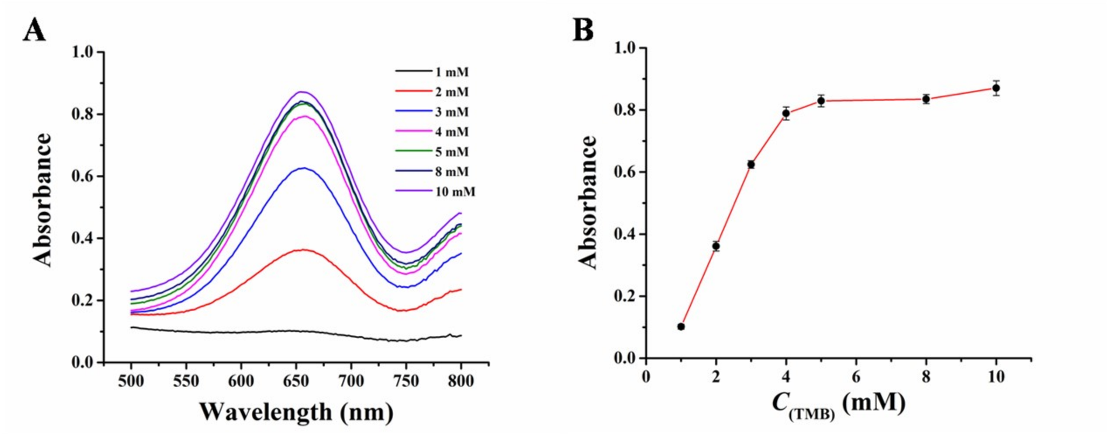

Figure S10. UV-vis absorption spectra of (A) concentration of TMB. Optimum conditions for xanthine response based on the Fe NPs nanozyme sensing platform. (B) concentration of TMB. The error bar represents the deviation of three determinations.

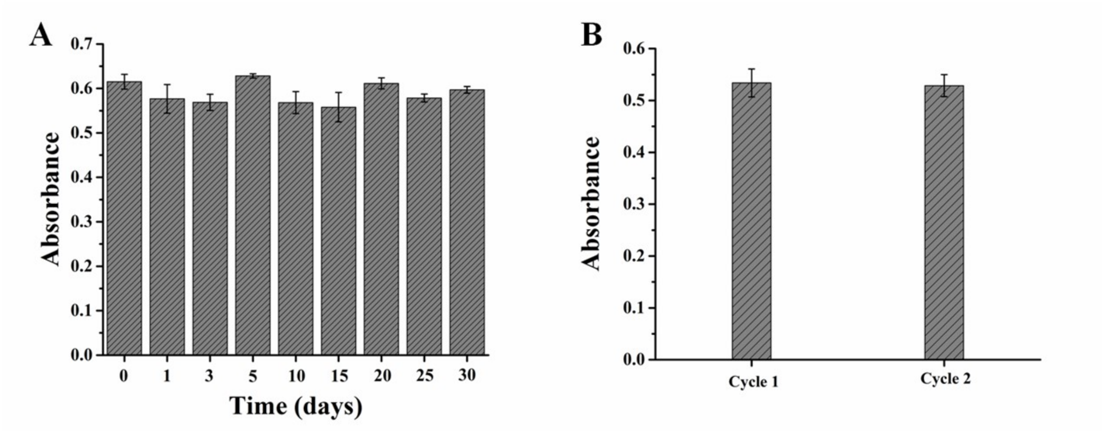

Figure S11. (A) The stability and (B) the reusability of the Fe NPs nanozyme for colorimetric detection of xanthine (50 μM). The error bar represents the deviation of three determinations.

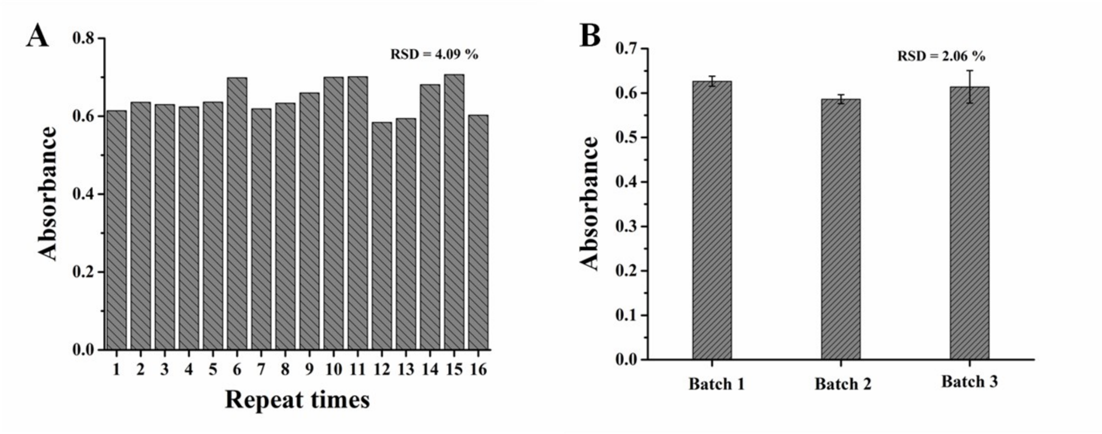

Figure S12. (A) The reproducibilty testing and (B) the batch-to-batch repeatability of the Fe NPs nanozyme for colorimetric detection of xanthine (50 μM).

Table S1. Catalytic factors of various peroxidase nanozymes

catalyst	substrate	K_m (mM)	V_{max} (10^{-8} M s^{-1})	reference
Fe NPs	H_2O_2	0.024	8.5	this work
	TMB	0.36	17.98	
HRP	H_2O_2	3.7	8.71	2
	TMB	0.434	10	
MoS_2	H_2O_2	0.0116	4.29	3
	TMB	0.525	5.16	
Au NPs	H_2O_2	61.34	0.663	4
	TMB	0.11	1.539	
Fe-MIL-88-NH_2	H_2O_2	0.206	7.04	5
	TMB	0.284	10.47	
Fe-PDA	H_2O_2	0.16	21.49	6
	TMB	0.4	20.59	
$MoSe_2$	H_2O_2	0.155	0.99	7
	TMB	0.014	0.56	
Au_{21} Pd_{79}	H_2O_2	5.89	8.19	8
	TMB	0.295	19.65	
Fe_3O_4	H_2O_2	2.995	0.9193	9
	TMB	31.20	1.614	
Fe–N–C SACs	H_2O_2	13.18	26.62	10
	TMB	0.96	132.58	
Fe-CDs	H_2O_2	0.58	4.23	11
	TMB	0.18	5.97	
Fe@MoS_2	H_2O_2	0.030	2.01	12
	TMB	/	/	
Fe SACs	H_2O_2	/	/	13
	TMB	0.156	0.219	
NO_2-MIL-101	H_2O_2	1.10	88.9	14
	TMB	9.01	150.3	

Table S2. The comparison of the proposed colorimetric methods with other approaches for xanthine detection.

Method	Linear range	Limit of detection	Reference
Photoluminescent	1-50 μM	0.34 μM	15
Electrochemical	1-100 μM	70 nM	16
Colorimetric	0.01-0.32 mM	1.964 μM	7
Colorimetric	0.01-0.5 mM	4.37 μM	17
Colorimetric	125 nM-6.0 μM	23 nM	18
Electrochemical	0.7-200.0 μM	28 nM	19
Colorimetric	0.001-0.05 mM	0.29 mM	20
Colorimetric	0.16-40 μM	0.016 μM	21
Electrochemical	0.10-20 μM	0.006 μM	22
Photoelectrochemical	0.04-90 μM	6.6 nM	23
Surface plasma resonance	0-3 μM	0.0127 μM	24
Electrochemical	0.8-450 μM	0.4 μM	25
Colorimetric	0.1-80 μM	0.034 μM	This work

Table S3. Assay results for xanthine detection in serum sample by the proposed method

serum samples	xanthine (μM) added	found (mean ± SD)	RSD (%)	recovery (%)
Sample 1	5.0	5.32 ± 0.28	5.3	106.4
	10.0	10.78 ± 0.39	3.6	107.8
	50.0	53.56 ± 2.51	4.7	107.1
Sample 2	5.0	4.98 ± 0.34	6.8	99.6
	10.0	10.92 ± 0.53	4.9	109.2
	50.0	51.53 ± 1.95	3.8	103.1
Sample 3	5.0	5.16 ± 0.19	3.7	103.2
	10.0	10.54 ± 0.42	4.0	105.4
	50.0	48.75 ± 2.12	4.3	97.5

References

1 L. Zhang, J. Wang, C. Zhao, F. Zhou, C. Yao and C. Song, *Sens. Actuators B Chem.*, 2022, **361**, 131750.

2 L. Gao, J. Zhuang, L. Nie, J. Zhang, Y. Zhang and N. Gu, Nat. *Nanotechnol.*, 2007, **2**, 577-583.

3 T. Lin, L. Zhong, L. Guo, F. Fu and G. Chen, *Nanoscale*, 2014, **6**, 11856-11862.

4 Q. Xue, X. Niu, P. Liu, M. Wang, Y. Peng and H. Peng, *Sens. Actuators B Chem.,* 2021, **334**, 129650.

5 Y.L. Liu, X.J. Zhao, X.X. Yang and Y.F. Li, *Analyst,* 2013, **138**, 4526-4531.

6 Y. Zhang, X. Gao, Y. Ye and Y. Shen, *Analyst*, 2022, **147**, 956-964.

7 X. Wu, T. Chen, J. Wang and G. Yang, *J. Mater. Chem. B,* 2018, **6**, 105-111.

8 S. Cai, Z. Fu, W. Xiao, Y. Xiong, C. Wang and R. Yang, *ACS Appl. Mater. Interfaces*, 2020, **12**, 11616-11624.

9 H. Dong, W. Du, J. Dong, R. Chen, F. Kong, W. Cheng, M. Ma, N. Gu and Y. Zhang, *Nature Commun.*, 2022, **13**, 5365.

10 S. Ding, J.A. Barr, Z. Lyu, F. Zhang and M. Wang, *Adv. Mater.*, 2023, 2209633.

11 R. Qin, Y. Feng, D. Ding, L. Chen and S. Li, *ACS Appl. Bio Mater.,* 2021, **4**, 5520-5528.

12 S.R. Ali and M. De, *ACS Appl. Mater. Interfaces*, 2022, **14**, 42940-42949.

13 J. Liu, L. Gong, H. Chen, J. Gui and X. Zhu, *ACS Appl. Nano Mater.*, 2023, **6**, 5879-5888.

14 W. Xu, Y. Kang, L. Jiao, Y. Wu and H. Yan, *Nano-Micro Lett.*, 2020,**12**, 184.

15 Q. Lu, J. Wang, B. Li, C. Weng, X. Li and W. Yang, *Anal. Chem.*, 2020, **92**, 7770-7777.

16 W. Zheng, J. Yao and Y. Zhao, *Anal. Chem.*, 2021, **93**, 13080-13088.

17 C. Hong, L. Guan, L. Huang, X. Hong and Z. Huang, *New J. Chem.,* 2021, **45**, 10459-10465.

18 W. Pu, H. Zhao, L. Wu and X. Zhao, *Microchim. Acta*, 2015, **182**, 395-400.

19 Y. Cui, J. Li, M. Liu, H. Tong, Z. Liu and J. Hu, *Microchim. Acta*, 2020, **187**, 589.

20 W. Shi, H. Fan, S. Ai and L. Zhu, *RSC Adv*., 2015, **5**, 32183-32190.

21 F. Qiao, J. Wang, S. Ai and L. Li, *Sens. Actuators B. Chem*., 2015, **216**, 418-427.

22 Y. Wang, H. Zhao, H. Song, J. Dong and J. Xu, *Microchim. Acta*, 2020, **187**, 543.

23 X. Chen, P. Li, C. Luo and C. Huang, *Chem. Electro. Chem.*, 2022, **9**, e202200237.

24 R. Kant, R. Tabassum and B.D. Gupta, *Biosens. Bioelectron.*, 2018, **99**, 637-645.

25 M. Roostaee and I. Sheikhshoaie, *J. Food Meas. Charact.*, 2022, **16**, 731-739.